https://ntrs.nasa.gov/search.jsp?R=19860002057 2020-03-20T16:12:07+00:00Z

NASA TM-84924

NASA Technical Memorandum 84924

NASA-TM-84924 19860002057

Stress Analyses of B-52 Pylon Hooks

William L. Ko and Lawrence S. Schuster

LIBRARY COPY

OCT 2 1 1985

LANGLEY RESEARCH CENTER
LIBRARY, NASA
HAMPTON, VIRGINIA

October 1985

NASA
National Aeronautics and
Space Administration

NASA Technical Memorandum 84924

Stress Analyses of B-52 Pylon Hooks

William L. Ko and Lawrence S. Schuster
Ames Research Center, Dryden Flight Research Facility, Edwards, California

1985

National Aeronautics and
Space Administration
Ames Research Center
Dryden Flight Research Facility
Edwards, California 93523

N86-11524 #

SUMMARY

The NASTRAN finite element computer program was used in the two-dimensional stress analysis of B-52 carrier aircraft pylon hooks: (1) old rear hook (which failed), (2) new rear hook (improved geometry), (3) new DAST rear hook (derated geometry), and (4) front hook. NASTRAN model meshes were generated by the aid of PATRAN-G computer program. Brittle limit loads for all the four hooks were established. The critical stress level calculated from NASTRAN agrees reasonably well with the values predicted from the fracture mechanics for the failed old rear hook. The NASTRAN-predicted stress at the critical point of the hook agrees very well with the strain gage data.

INTRODUCTION

The NASA B-52-008 carrier aircraft has been used to carry various types of test vehicles for high-altitude drop tests. Typical test vehicles carried by the B-52 have been the X-15 (35,250 lb without drop tanks, 51,600 lb with drop tanks), HL-10 lifting body (15,380 lb), HiMAT (3528 lb plus 4000-lb adapter), DAST (2500 lb with 4000-lb adapter), and solid rocket booster and drop test vehicle (SRB/DTV, 49,000 lb). The test vehicle or adapter is attached to the B-52 pylon through one front hook and two rear hooks (see fig. 1 for the SRB/DTV). There are two sets of rear hooks; one set is for carrying longer test vehicles such as the X-15 and SRB/DTV; the other set is for carrying shorter test vehicles such as drones for aerostructural testing (DAST). The previously established limits for vertical loads on the front and rear hooks are 37,700 lb and 57,600 lb, respectively. The SRB/DTV is a scale model of the SRB and is used for testing the performance of the SRB main parachute system. The DTV is 611 in long and weighs about 48,267 lb. The SRB/DTV weight will induce static vertical loads of 13,908 lb at the front hook and 17,180 lb at each rear hook. Although the static hook loads were well below the limit loads, the two rear hooks failed during towing of the B-52 carrying SRB/DTV on a relatively smooth taxiway (very small dynamic loading), after cancellation of the first of the new series of SRB/DTV drop tests because of unfavorable weather conditions. The initial failure occurred in the outboard rear hook, resulting in an increased load on the inboard rear hook and causing it to fail as well (fig. 2). The microscopic observations of the fracture surfaces of the two failed rear hooks by Nelson[1] revealed that microsurface cracks existed at the rounded corners (or hook notches) of both hooks (figs. 2 and 3). These surface cracks became unstable and propagated because the stress levels in the vicinity of the crack sites exceeded the critical values associated with the crack sizes.

These stress levels far exceeded the values predicted by the conventional "strength-of-materials" analysis and raised serious doubt about the load limits established previously (pre-NASTRAN era) for all B-52 pylon hooks based on the

---

[1]"Failure Analysis of the Aft Hooks, B-52 Special Project Aircraft," unpublished memorandum by H.C. Nelson, Materials and Test Engineering Branch, NASA Ames Research Center, 1983.

strength-of-materials stress analysis. It was therefore necessary to repeat the stress analysis of all B-52 pylon hooks using a refined method, such as the finite element method, and to reestablish the limit loads for all B-52 pylon hooks.

This report presents the results of stress analyses of the B-52 pylon hooks using the NASTRAN finite element computer code and establishes the brittle limit loads for all hooks. In addition, the stress level calculated from NASTRAN for the critical point at the rounded corner of the old rear hook is compared with the values predicted by the fracture mechanics.

SYMBOLS

a	maximum depth (semiminor axis) of a semielliptic surface crack
c	half crack length (semimajor axis) of a semielliptic surface crack
$E(k)$	complete elliptic integral of the second kind
K_I	mode I stress intensity factor
k	modulus of elliptic function, $k^2 = 1 - \left(\frac{a}{c}\right)^2$
M_F	surface stress intensity magnification factor
P	hook vertical load
P_U	hook load that causes $\sigma_T \mid_{max}$ to reach σ_U
P_Y	hook load that causes $\sigma_T \mid_{max}$ to reach σ_Y
P_S	hook load that causes $\tau_{xy} \mid_{max}$ to reach τ_U
Q	surface flaw shape and plasticity factor
θ	angular coordinate
σ_∞	applied stress
σ_T	tangential stress along hook inner boundary or across the hook depth
σ_U	ultimate stress
σ_Y	yield stress
τ_{xy}	shear stress
τ_U	ultimate shear stress

ϕ angular coordinate associated with a semielliptical surface crack

$[\,]\big|_{max}$ maximum value of $[\,]$

SURFACE CRACKS

For a semiinfinite solid containing a semielliptical surface crack under Mode I deformation (loading axis is perpendicular to the crack plane, fig. 4), the stress intensity factor K_I at the deepest penetration (point A, fig. 4) of the surface flaw is given in reference 1.

$$K_I = M_F \sigma_\infty \sqrt{\frac{\pi a}{Q}} \tag{1}$$

where σ_∞ is the applied stress, a is the maximum crack depth (semiminor axis of ellipse), and M_F is the surface stress intensity magnification factor given by

$$M_F = 1.0 + 0.12\left(1 - \frac{a}{2c}\right)^2 \tag{2}$$

$$\longrightarrow 1.12 \text{ as } \frac{c}{a} \longrightarrow \infty \qquad \text{(two-dimensional-edge crack case)}$$

where c is the half-crack length (semimajor axis of ellipse). Lastly, Q in equation (1) is the surface flaw shape and plasticity factor given by

$$Q = [E(k)]^2 - 0.212\left(\frac{\sigma_\infty}{\sigma_Y}\right)^2 \tag{3}$$

where E(k) is the complete elliptic integral of the second kind, namely,

$$E(k) = \int_0^{\frac{\pi}{2}} \sqrt{1 - k^2 \sin^2 \phi}\, d\phi \tag{4}$$

$$k^2 = 1 - \left(\frac{a}{c}\right)^2$$

and σ_Y in equation (3) is the yield stress of the material.

The combination of equations (1) and (3), σ_∞ can be expressed as

$$\frac{\sigma_\infty}{\sigma_Y} = \frac{E(k)}{\sqrt{\pi a\left(\frac{M_F \sigma_Y}{K_I}\right)^2 + 0.212}} \tag{5}$$

Equation (5) can be used to calculate the critical values of σ_∞ at which the surface crack of a given size will propagate if σ_Y and the critical value of K_I of the material are known.

Alternatively, if we rewrite equation (5) in the following form

$$a = \frac{K_I^2}{\pi M_F^2 \sigma_Y^2}\left\{\left[E(k)\,\frac{\sigma_Y}{\sigma_\infty}\right]^2 - 0.212\right\} \tag{6}$$

we can estimate the critical crack size for a given stress level σ_∞, σ_Y, and the critical value of K_I.

For the 4340 alloy steel used for the two failed rear hooks, the critical value of K_I at the state of incipient crack propagation is about $K_I = 50{,}000$ (lb/in^2) $\sqrt{\text{in}}$ and σ_Y is about 225×10^3 lb/in^2 as obtained from figure 5.

Outboard Rear Hook

The size of the surface crack in the outboard rear hook at the time of fracture was estimated as

$$a = 0.038 \text{ in} \tag{7}$$

$$c = 2a \tag{8}$$

which gives

$$M_F = 1.0675 \tag{9}$$

$$k = 0.8660 \tag{10}$$

$$E(k) = 1.2111 \tag{11}$$

for a semielliptic surface crack.

Since the crack size is very small compared with the thickness and the notch curvature of the hook, the problem near the crack site may be considered as a semi-infinite solid containing a surface crack. If we assume that the surface crack is semielliptic, then equation (5) can be used to estimate the value of σ_∞ at the instant of hook fracture. For the hook, σ_∞ will be the tangential stress along the circular notch boundary near the crack site and normal to the crack plane. When the numerical values given above are used, equation (5) gives

$$\sigma_\infty = 158{,}203 \text{ lb/in}^2 \tag{12}$$

which is the stress level reached near the crack site of the outboard rear hook at the moment of its catastrophic failure.

Inboard Rear Hook

For the inboard rear hook, the surface crack size at the instant of rapid crack propagation was estimated as

$$a = 0.031 \text{ in} \tag{13}$$

$$c = a \tag{14}$$

which gives

$$M_F = 1.03 \tag{15}$$

$$k = 0 \tag{16}$$

$$E(k) = 1.5708 \tag{17}$$

for a semicircular surface crack, and in light of those values, equation (5) gives

$$\sigma_\infty = 232{,}831 \text{ lb/in}^2 \tag{18}$$

for the stress level reached near the crack site of the inboard rear hook at the instant of fracture.

STRESS ANALYSIS

Stress analysis was performed for the following B-52 pylon hooks: (1) old rear hook (which failed), (2) new rear hook (improved geometry), (3) new DAST hook (derated geometry), and (4) the front hook. The NASTRAN finite element computer program (ref. 2) was used in the two-dimensional stress analysis. In generating the meshes for the NASTRAN models of the hooks, the PATRAN-G computer program (ref. 2) was used. This computer program allows the analyst to easily generate a finite-element mesh for any given geometric shape. Working interactively using engineering drawings, the outline of the structure is generated and displayed on a graphics terminal. Then the structure is further divided into zones, called patches (or subregions), that are bounded by lines with either geometric significance (such as thickness changes) or finite-element significance (such as changes in desired mesh density). After all the patches are defined, a finite-element mesh is chosen for each patch. The topological zoom technique is used to provide transitions in mesh density while preserving complete connectivity. All structural node locations and element definitions (connectivity) are generated from the basic structural dimensions and the finite-element mesh instructions for each patch. Finally, a "neutral file" is produced which contains all the finite-element definitions. The neutral file data are then converted to NASTRAN-GRID and CXXXX (element connection) cards by another program called PATNAS. NASTRAN executive and case control decks, pertinent loads, constraints, and material properties are added to the output file from PATNAS before beginning the NASTRAN analysis. Plots of the resulting finite-element mesh generated by PATRAN-G are used to interpret the results from the NASTRAN analysis.

Old Rear Hook

Figure 6 shows the geometry of the old rear hook which failed. For the stress analysis, only the lower portion of the hook was modeled. The PATRAN-G computer program was used to divide into patches the region to be analyzed (fig. 7). Within each patch refined meshes were generated. In connecting a patch with a coarse mesh to a patch with a fine mesh, some triangular elements were introduced so that there would be no floating nodes.

Figure 8 shows the NASTRAN model for the old rear hook. The model has 1667 grid points, 1525 CQUAD4 elements, and 73 CTRIA3 elements. The applied load was the static load of P = 17179.53 lb, with 1.5 in of moment arm. The upper horizontal boundary was constrained in such a way that there would be no vertical displacement.

Figure 9 shows the distribution of the calculated tangential stress σ_T (positive in tension) along the inner boundary of the old rear hook. The figure shows that σ_T reached its peak value $\sigma_T \big|_{max} = 172{,}200$ lb/in^2 at point C (a critical point) located at 36.25° measured from a horizontal line. The location of C is close to the sites of the surface cracks shown in figure 2. The value $\sigma_T \big|_{max} = 172{,}200$ lb/in^2 lies between the two values of the critical stresses calculated from the fracture mechanics (eqs. (12) and (18)). This implies that if a surface crack of the size comparable to the observed sizes exists at point C (eqs. (7), (8), (13), and (14)), it is likely that the old rear hook could fail even if it were under the static loading. Figure 10 shows the distribution of the peak σ_T inside the hook. This peak σ_T line starts from point C, making a 36.35° inclination near point C, rapidly turning to about 20° inclination across the depth of the hook. This peak σ_T line agrees reasonably well with the actual fracture lines (although they are somewhat curved near the outer hook boundaries) as shown in figure 2. In addition, in figure 10, distribution of σ_T calculated from strength-of-materials (elementary theory) is shown in a broken line for comparison. Notice that the value of $\sigma_T \big|_{max}$ at point C calculated from NASTRAN is 3.15 times that predicted from the elementary theory (that is, stress concentration factor 3.15). This shows the inadequacy of the elementary theory for the hook geometry, which is not a straight bar, and raises serious doubt about the values of the limit loads previously established for all the B-52 pylon hooks based on the elementary theory which ignored stress concentration effect. At point D′, which is located at the upper end of the notch curvature (fig. 11), the stress concentration factor decreases to 2.11. At point B′, which is located in the hook straight region (fig. 12), the predictions from the two theories become close, the stress concentration factor comes down to 1.09, and the stress concentration effect practically diminishes. Figure 13 shows the distributions of shear stress τ_{xy} along three cross-sectional lines θ = 0°, 5°, and 10° of the hook. The peak τ_{xy} falls on the θ = 5° line, giving $\tau_{xy} \big|_{max} = 27{,}600$ lb/in^2 for P = 17179.53 lb loading. For the 4340 alloy steel (ref. 4) used in the old rear hook, we have

$$\text{Ultimate tensile stress } \sigma_U = 260 \text{ to } 280 \times 10^3 \text{ lb/in}^2 \tag{19}$$

$$\text{Yield stress } \sigma_Y = 225 \times 10^3 \text{ lb/in}^2 \tag{20}$$

$$\text{Ultimate shear stress } \tau_U = 156 \times 10^3 \text{ lb/in}^2 \tag{21}$$

Based on these values, the $\sigma_T \big|_{max}$ at the critical point C, and the $\tau_{xy} \big|_{max}$ on the $\theta = 5°$ line, the following rear hook loads can be established.

1. P_U, the hook load which will cause $\sigma_T \big|_{max}$ at point C to reach σ_U

$$P_U = \frac{\sigma_U}{\sigma_T \big|_{max}} P = \frac{260,000}{172,200} \times 17179.53 \tag{22}$$

$$P_U = 25,939 \text{ lb} \tag{23}$$

2. P_Y, the hook load which will cause $\sigma_T \big|_{max}$ at point C to reach σ_Y

$$P_Y = \frac{\sigma_Y}{\sigma_T \big|_{max}} P = \frac{225,000}{172,200} \times 17179.53 \tag{24}$$

$$P_Y = 22,447 \text{ lb} \tag{25}$$

3. P_S, the hook load which will cause $\tau_{xy} \big|_{max}$ to reach τ_U

$$P_S = \frac{\tau_U}{\tau_{xy} \big|_{max}} P = \frac{156,000}{172,200} \times 17179.53 \tag{26}$$

$$P_S = 97,102 \text{ lb} \tag{27}$$

It is seen that the hook is likely to fail in tension rather than in shear. The value of P_U (eq. (23)) calculated from equation (22) is based on the assumption of brittle fracture. If the plastic deformation is allowed, the value of P_U could be increased considerably. (The previously established old rear hook limit load was 57,600 lb, which was based on the ductile fracture.)

New Rear Hook

Figure 14 shows the geometry of the new rear hook. Notice that the hook notch radius and the hook width have been increased to reduce the stress concentration at the hook notch boundary. In figure 14, the boundary of the old rear hook (broken line) is shown for comparison. The region of analysis was extended up to the pinhole region. Because of the hook contour shape, PATRAN patches were carefully generated to avoid the creation of overdistorted meshes. The PATRAN patches for the new rear hook are shown in figure 15. Note that the hook thickness transition line was used as the boundary for some patches. Figure 16 shows the NASTRAN model of the new rear hook. The model has 2083 grid points, 1926 CQUAD4 elements, and 14 CTRIA3 elements. The applied load was the static load of P = 17,179.53 lb with a 2-in moment arm. The vertical displacement of the straight regions of the upper boundary of the model was set to zero. No constraint was applied to the pinhole boundary. Figure 17 shows the distribution of tangential stress σ_T along the inner boundary of the hook. The σ_T stress distribution is more uniform in the circular notch

region as compared to the old rear hook. It is seen that σ_T reached its peak value of $\sigma_T \big|_{max} = 100{,}400$ lb/in^2 at the 28.75° point measured from a horizontal line, and that σ_T has an abrupt change in value at the point of thickness transition. Figure 18 shows the distribution of σ_T along the 28.75° line across the hook depth predicted from both NASTRAN and the elementary theory. The stress concentration factor at the critical point C ($\sigma_T \big|_{max}$ point) is 2.61 as compared with 3.15, the peak stress concentration factor for the old rear hook. At point B, which lies on the horizontal line passing through the center of radius of curvature of the hook notch (fig. 19), the stress concentration factor is reduced to 1.86. Figure 20 shows the distribution of shear stress τ_{xy} across three cross sections, $\theta = 0°$, 5°, and 10°. For the $\theta = 0°$ cross section, τ_{xy} reached the highest value of $\tau_{xy} \big|_{max} = 20{,}034$ lb/in^2.

For the material AMAX MP35N alloy[2] used in the new rear hook, we have

$$\sigma_U = 250 \times 10^3 \text{ lb/in}^2 \tag{28}$$

$$\sigma_Y = 235 \times 10^3 \text{ lb/in}^2 \tag{29}$$

$$\tau_U = 141 \times 10^3 \text{ lb/in}^2 \tag{30}$$

If the same definitions are used for P_U, P_Y, and P_S, as in the case of the old rear hook, the following hook loads can be established.

1.

$$P_U = \frac{\sigma_U}{\sigma_T \big|_{max}} P = \frac{250{,}000}{100{,}400} \times 17179.53 \tag{31}$$

$$P_U = 42{,}778 \text{ lb} \tag{32}$$

2.

$$P_Y = \frac{\sigma_Y}{\sigma_T \big|_{max}} P = \frac{235{,}000}{100{,}400} \times 17179.53 \tag{33}$$

$$P_Y = 40{,}211 \text{ lb} \tag{34}$$

3.

$$P_S = \frac{\tau_U}{\tau_{xy} \big|_{max}} P = \frac{141{,}000}{20{,}034} \times 17179.53 \tag{35}$$

$$P_S = 121{,}116 \text{ lb} \tag{36}$$

Thus the mode of failure of the new rear hook will be tensile failure rather than shear failure.

---

[2]AMAX Specialty Corporation, Ten Road, Cleveland, OH 44117.

In order to estimate the critical size of a surface crack which the new rear hook can carry under the static loading of 17179.53 lb, two assumptions will be made for the shape of the crack: (1) semieliptical crack with $\frac{a}{2c} = \frac{1}{4}$ (fig. 4) and (2) semicircular crack with $\frac{a}{2c} = \frac{1}{2}$ (fig. 4).

Case 1: Semielliptical Crack $\frac{a}{2c} = \frac{1}{4}$

Substituting equations (9) through (11) into equation (6) and using $\sigma_Y = 235 \times 10^3$ lb/in^2 and $K_I = 124 \times 10^3$ lb/in^2 for the AMAX MP35N alloy steel, we have

$$a = 0.0778\left(\frac{7.4255}{\sigma_\infty^2 \times 10^{-10}} - 0.212\right) \tag{37}$$

Taking $\sigma_\infty = \sigma_T \Big|_{max} = 100{,}400$ lb/in^2, equation (37) yields

$$a = 0.56 \text{ in} \tag{38}$$

which is 14.64 times the size of crack a = 0.038 in the old outboard rear hook carried at the time of fracture.

Case 2: Semicircular Crack $\frac{a}{2c} = \frac{1}{2}$

Substitution of equations (15) through (17) and the values of σ_Y and K_I into equation (6) yields

$$a = 0.0835\left(\frac{12.4913}{\sigma_\infty^2 \times 10^{-10}} - 0.212\right) \tag{39}$$

Again, using $\sigma_\infty = \sigma_T \Big|_{max} = 100{,}400$ lb/in^2, equation (39) gives

$$a = 1.02 \text{ in} \tag{40}$$

which is 32.82 times the size of crack a = 0.031 in which the old inboard rear hook carried at the instant of its fracture. Thus the new rear hook has much higher structural performance than the old rear hook.

New DAST Rear Hook

Figure 21 shows the geometry of the new DAST rear hook which has a larger radius of curvature at the hook notch for the reduction of stress concentration. In the figure, the contour of the existing DAST hook is shown for comparison. The PATRAN patches for the new DAST hook is shown in figure 22. The hook was modeled up to the

main pinhole region. The pin was ignored. Figure 23 shows the new DAST rear hook NASTRAN model which has 2089 grid points, 1935 CQUAD4 ele-ments, and 4 CTRIA3 elements. The applied load was P = 10,000 lb with a 1.5-in moment arm. The constraints applied at the upper boundary of the model were the same as for the new rear hook. Figure 24 shows the distribution of stress σ_T along the inner boundary of the hook. The critical point is located at the 11.25° point where σ_T reached its peak value of $\sigma_T \big|_{max} = 100{,}700$ lb/in^2.

Figure 25 shows the distribution of σ_T along the 11.25° line across the depth of the hook. The stress concentration factor at the critical point C is 1.96. Figure 26 shows the distributions of shear stress τ_{xy} along $\theta = 0°$, 5°, and 10° cross-sectional lines. The peak shear stress $\tau_{xy} \big|_{max} = 23{,}260$ lb/in^2 falls on the $\theta = 0°$ line.

For the 4140 alloy steel (ref. 4) used in the DAST rear hook, we have

$$\sigma_U = 160 \text{ to } 180 \times 10^3 \text{ lb/in}^2 \tag{41}$$

$$\sigma_Y = 145 \times 10^3 \text{ lb/in}^2 \tag{42}$$

$$\tau_U = 135 \times 10^3 \text{ lb/in}^2 \tag{43}$$

Thus

1.

$$P_U = \frac{\sigma_U}{\sigma_T \big|_{max}} P = \frac{160{,}000}{100{,}700} \times 10{,}000 \tag{44}$$

$$P_U = 15{,}889 \text{ lb} \tag{45}$$

2.

$$P_Y = \frac{\sigma_Y}{\sigma_T \big|_{max}} P = \frac{145{,}000}{100{,}700} \times 10{,}000 \tag{46}$$

$$P_Y = 14{,}399 \text{ lb} \tag{47}$$

3.

$$P_S = \frac{\tau_U}{\tau_{xy} \big|_{max}} P = \frac{135{,}000}{23{,}260} \times 10{,}000 \tag{48}$$

$$P_S = 58{,}040 \text{ lb} \tag{49}$$

Thus the new DAST hook will have tensile failure rather than shear failure.

The geometry of the old DAST rear hook is quite similar to that of the old rear hook, both of which have the same radii of curvature at their inner circular corners. Therefore, the stress concentration factor at the critical point of the old

DAST rear hook will be approximately 3.15. Although the stress concentration factor at the critical point of the new DAST rear hook is only 1.96 (62 percent of 3.15), the value of $\sigma_T \big|_{max}$ of the new DAST rear hook is still as high as 90 percent of that of the old DAST rear hook because of the reduction in the moment of inertia of the new DAST rear hook due to the loss of some material in the inner circular corner region (fig. 21).

Front Hook

The geometry of the front hook is shown in figure 27. The lower part of the hook is separated into two parts by the groove. In the stress analysis, the lower split two regions were fused together and were considered as a single region with one thickness. The groove boundary line was then used as a thickness transition line. The PATRAN patches for the front hook are shown in figure 28. Notice that the thickness transition line was used as the boundary for some patches. Figure 29 shows the front hook NASTRAN model which has 1691 grid points, 1523 CQUAD4 elements, and 52 CTRIA3 elements. The horizontal regions of the upper boundary of the NASTRAN model were so constrained that there will be no vertical displacement. Also, the locations of points A and B at the boundary of the pinhole were fixed to simulate the pin effect. Figure 30 shows the distribution of the tangential stress σ_T at the hook inner boundary. The peak value $\sigma_T \big|_{max} = 73{,}522$ lb/in^2 is located at the 26.25° point measured from a horizontal line. Figure 31 shows the distributions of σ_T along the 26.25° line across the hook depth calculated from NASTRAN and the elementary theory. The stress concentration factor at the critical point C is 2.02. Finally, the distributions of shear stress τ_{xy} along $\theta = 0°$, 5°, and 10° cross-sectional lines are shown in figure 32. The $\theta = 0°$ cross section experienced highest shear with $\tau_{xy} \big|_{max} = 22{,}838$ lb/in^2.

For the INCONEL 718 material (ref. 5) used in the front hook,

$$\sigma_U = 175 \text{ to } 190 \times 10^3 \text{ lb/in}^2 \tag{50}$$

$$\sigma_Y = 135 \times 10^3 \text{ lb/in}^2 \tag{51}$$

$$\tau_U = 86 \times 10^3 \text{ lb/in}^2 \tag{52}$$

Then,

1.

$$P_U = \frac{\sigma_U}{\sigma_T \big|_{max}} P = \frac{175{,}000}{73{,}522} \times 10{,}000 \tag{53}$$

$$P_U = 23{,}802 \text{ lb} \tag{54}$$

2.

$$P_Y = \frac{\sigma_Y}{\sigma_T \big|_{max}} P = \frac{135{,}000}{73{,}522} \times 10{,}000 \tag{55}$$

$$P_Y = 18{,}362 \text{ lb} \tag{56}$$

$$P_S = \frac{\tau_U}{\tau_{xy}\,|\,_{max}} P = \frac{86,000}{22,838} \times 10,000 \tag{57}$$

$$P_S = 37,993 \text{ lb} \tag{58}$$

From equations (54) and (58), it is seen that the front hook will fail in tension rather than in shear. It must be mentioned that the value of P_U (eq. (54)) calculated from equation (53) is based on the assumption of brittle fracture. If the plastic deformation is allowed, the value of P_U could be raised considerably. (The previously established front hook limit load was 37,700 lb, which was based on the ductile fracture.)

Load-Stress Curves

Figure 33 shows plots of the hook load as a function of the maximum tangential tensile stress $\sigma_T\,|\,_{max}$ (at the critical point C) for the four hooks analyzed. The small arrow at each curve points to the location of the brittle failure point (that is, assuming no growth of the plastic zone around the critical point C). The curve with the lower slope gives higher hook-load carrying capacity (that is, higher structural efficiency) under the same level of $\sigma_T\,|\,_{max}$. The new rear hook is the most efficient of the four hooks. The strain-gauge-measured data for the front hook and the new rear hook[3] are also shown for comparison. The excellent agreement between the NASTRAN predictions and the strain gauge data implies that the NASTRAN modeling was almost perfect. For the front hook, the strain gauges were located in the straight region of the inner hook boundary as shown in figure 27; then by the aid of the stress plot shown in figure 30, $\sigma_T\,|\,_{max}$ was calculated from $\sigma_T\,|\,_{max}$ = 2.118 × strain gauge stress. For the rear hook, strain gauges were located at the critical point. The peak data point for the new rear hook lying beyond the brittle failure point suggests that the plastic zone was developed around the critical point C, and thus the new rear hook could actually carry loads higher than the brittle failure point without failure.

CONCLUSIONS

The NASTRAN finite-element computer program was used in the stress analysis of the old rear hook, the new rear hook, the new DAST rear hook, and the front hook. The highlights of the results of the NASTRAN analysis are summarized as follows.

1. For the old rear hook, the tensile stress level in the vicinity of the crack site (calculated from NASTRAN) was comparable to the Mode I failure stress predicted from the fracture mechanics.

[3]Data for the new rear hook were obtained by G.R. Swanson, NASA Marshall Space Flight Center.

2. For all the hooks analyzed, NASTRAN predicted much higher tangential stresses along the hook inner circular corner than those predicted from the elementary theory.

3. All the hooks will fail in tension rather than in shear.

4. The hook loads calculated based on NASTRAN are summarized in Table 1.

5. The hook loads P_U, P_Y for the old rear hook and °for the front hook based on NASTRAN are much less than the previously established limit loads.

6. The predicted stress at the critical point of the hook agrees very nicely with the strain gage measured values.

National Aeronautics and Space Administration
Ames Research Center
Dryden Flight Research Facility
Edwards, California, August 1, 1983

REFERENCES

1. Swedlow, J.L., ed.: The Surface Crack: Physical Problems and Computational Solutions. ASME Winter Annual Meeting, New York, N.Y., Nov. 26-30, 1972.

2. The NASTRAN User's Manual. NASA SP-222(05), 1978.

3. PATRAN Release Notes, Release 1.6. PDA/PATRAN-G, PDA Engineering, July 1984.

4. Aerospace Structural Metals Handbook. Volume 1, Ferrous Alloys. Metals and Ceramics Information Center, Battelle's Columbus Laboratories, Columbus, Ohio, 1982.

5. Aerospace Structural Metals Handbook. Volume 5, Nonferrous Alloys. Dept. of Defense, Mechanical Properties Data Center, 1981.

TABLE 1. — HOOKLOADS CALCULATED BASED ON NASTRAN

Hook	Stress concentration factor	Location of critical point, deg	P_U, lb	P_Y, lb	P_S, lb
Old rear hook	3.15	36.25	25,939	22,447	97,102
New rear hook	2.61	28.75	42,778	40,211	121,116
New DAST rear hook	1.96	11.25	15,889	14,399	58,040
Front hook	2.02	26.25	23,802	18,362	37,993

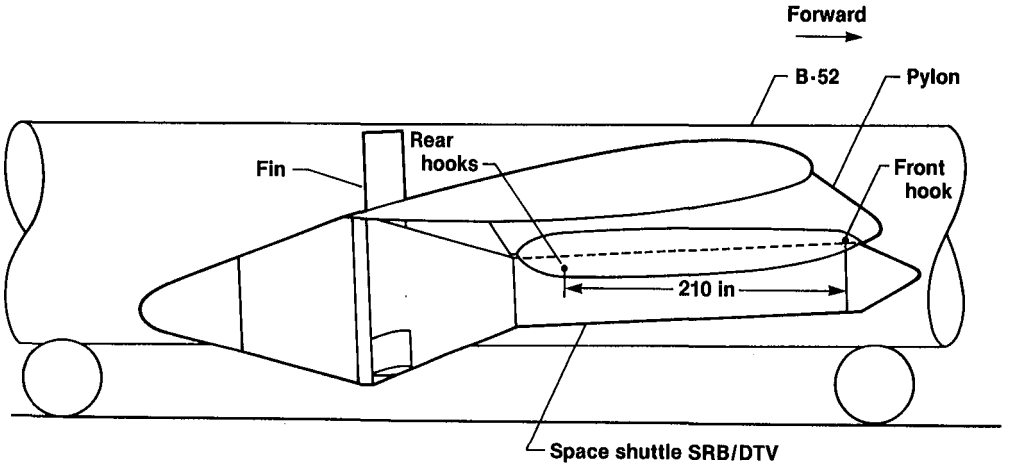

Figure 1. Geometry of space shuttle SRB/DTV attached to B-52 pylon. View looking inboard to right side of B-52 and DTV.

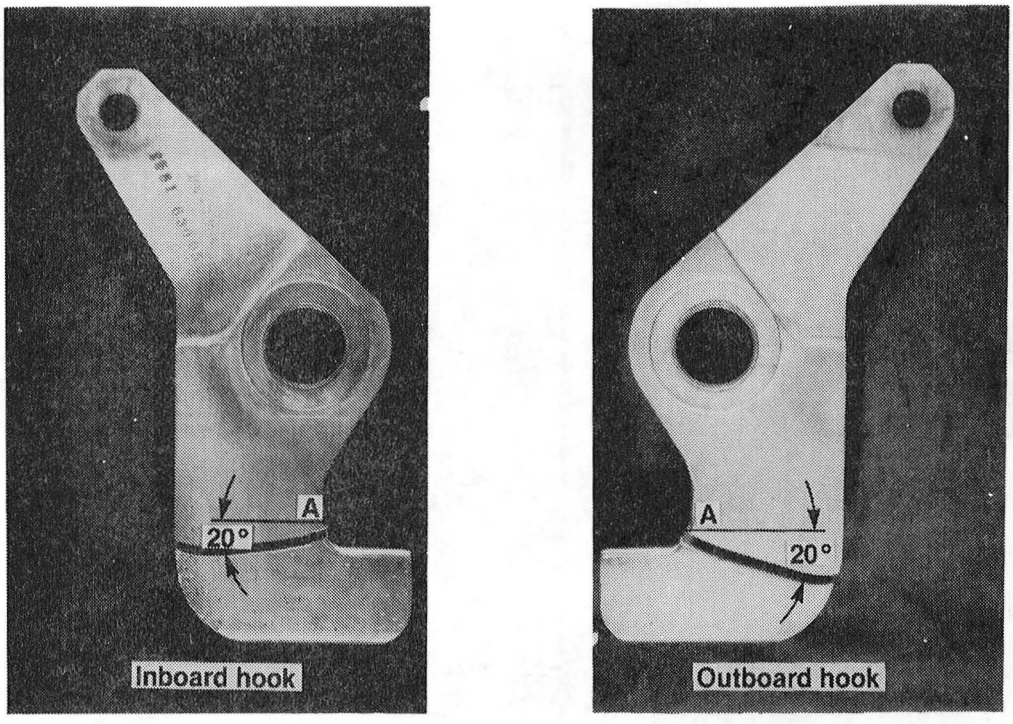

Figure 2. Fractured B-52 pylon rear hooks (A indicates the primary crack initiation sites).

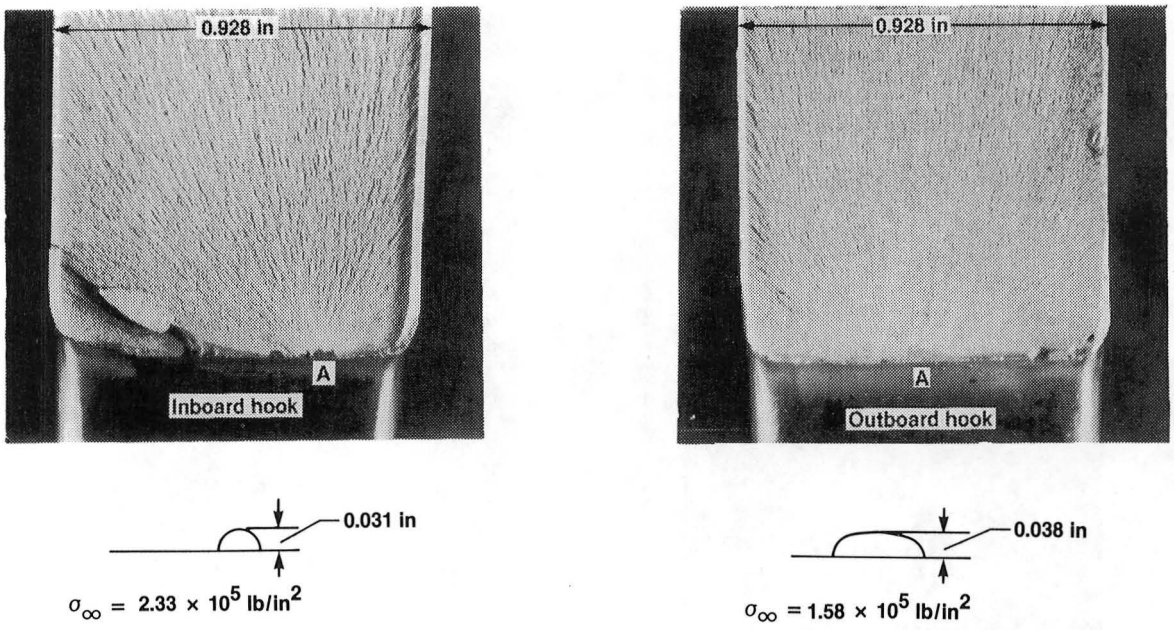

Figure 3. Fracture surfaces of B-52 pylon rear hooks (A indicates the primary crack initiation sites).

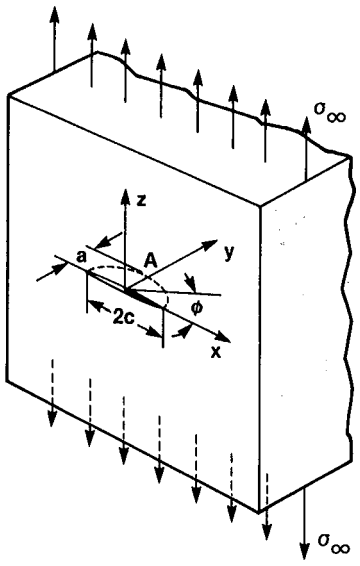

Figure 4. Semielliptical surface crack in a semiinfinite solid under mode I deformation.

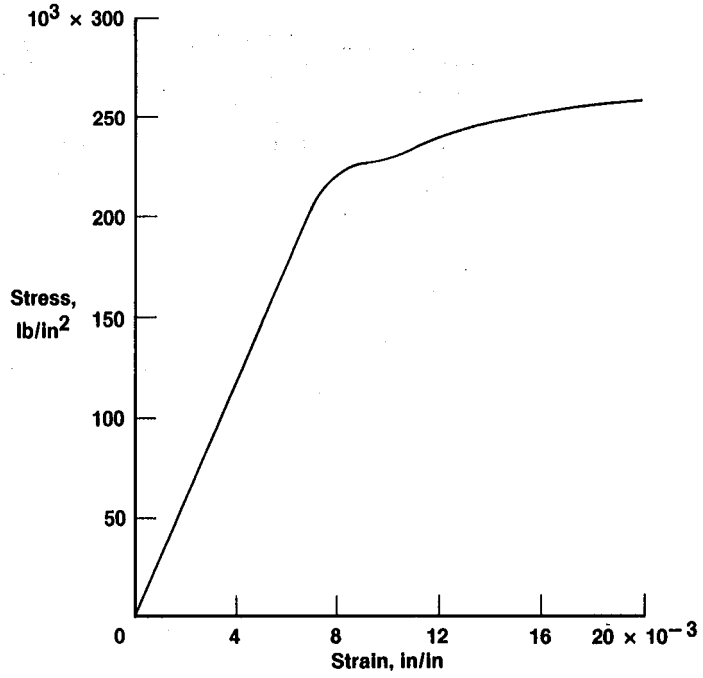

Figure 5. Stress-strain curve at room temperature for 4340 alloy steel.

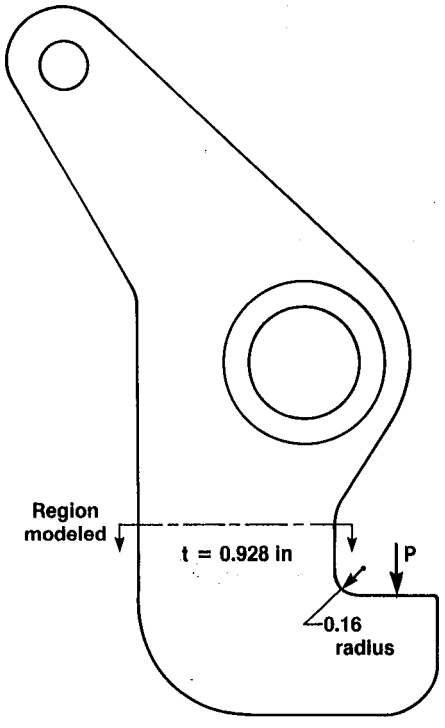

Figure 6. Geometry of B-52 pylon rear hook.

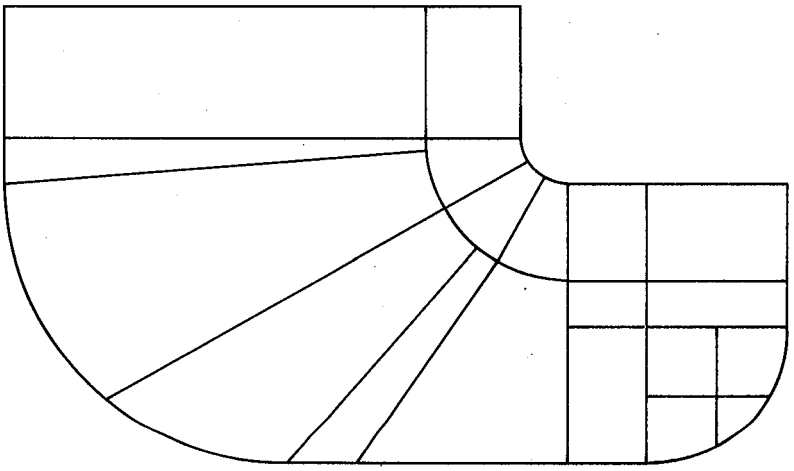

Figure 7. PATRAN patches (subregions) for generating meshes for the old rear hook NASTRAN model.

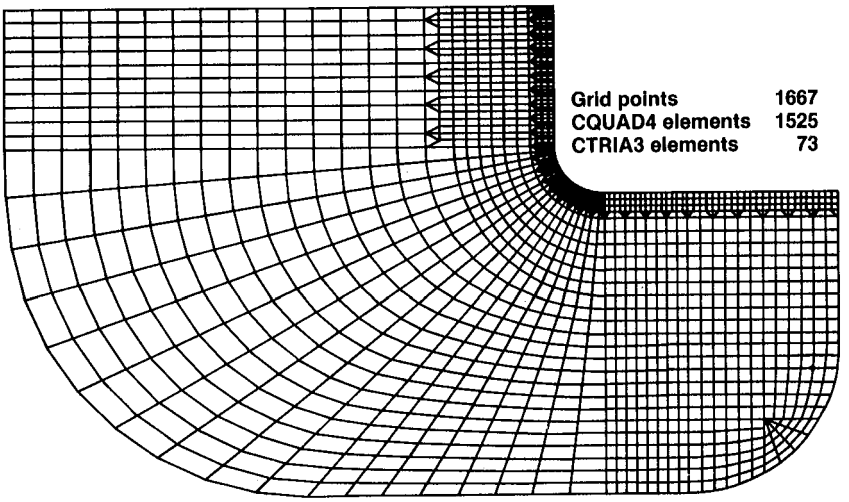

Figure 8. Old rear hook NASTRAN model.

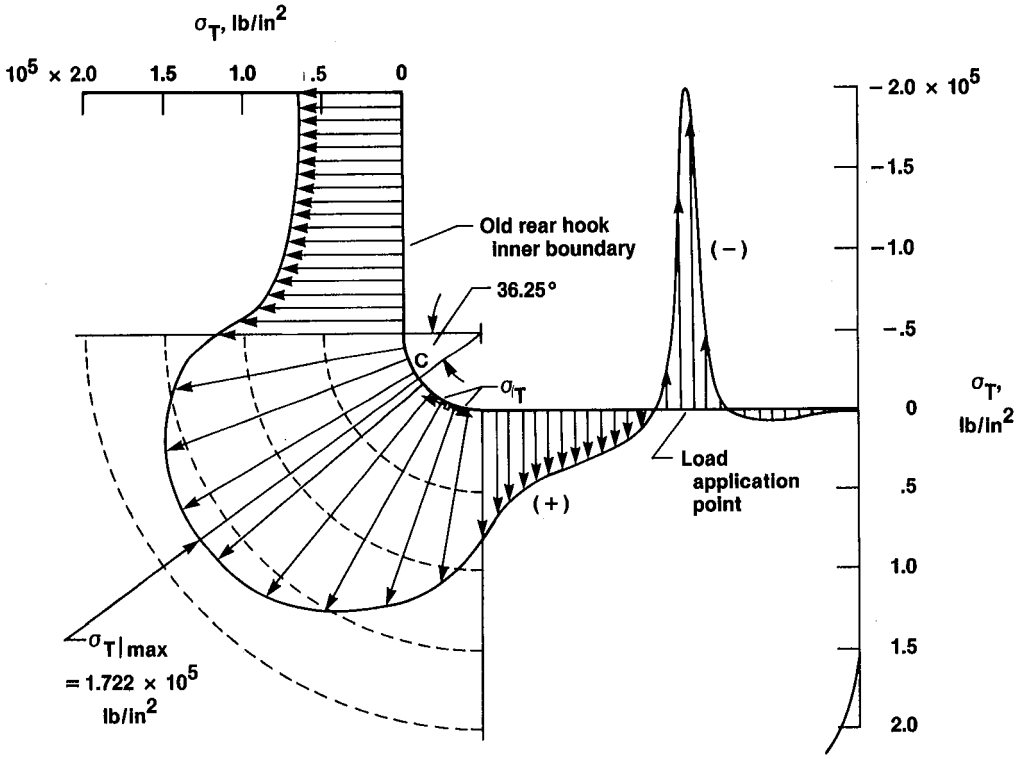

Figure 9. Distribution of tangential stress σ_T along inner boundary of the old rear hook (P = 17,179.53 lb).

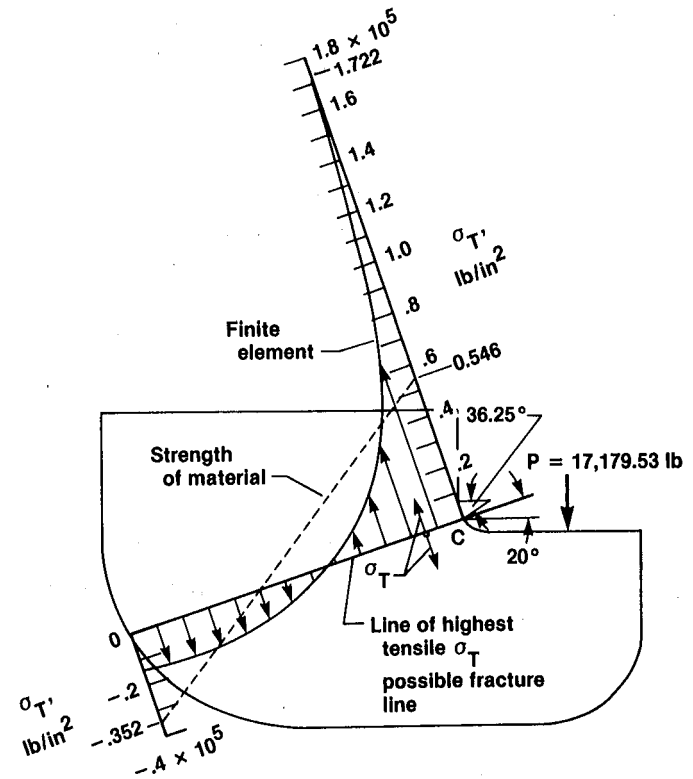

Figure 10. Distribution of σ_T along 20° line (old rear hook, P = 17,179.53 lb).

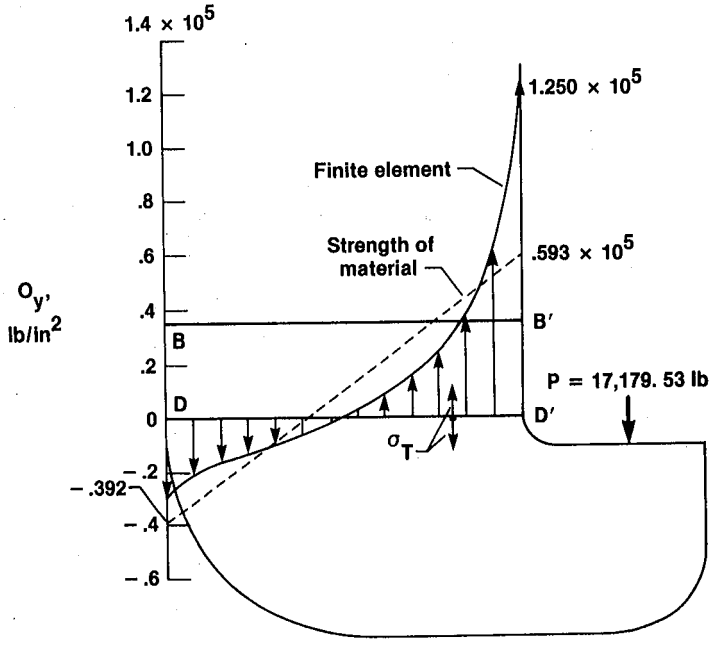

Figure 11. Distribution of σ_T along D-D' (old rear hook, P = 17,179.53 lb).

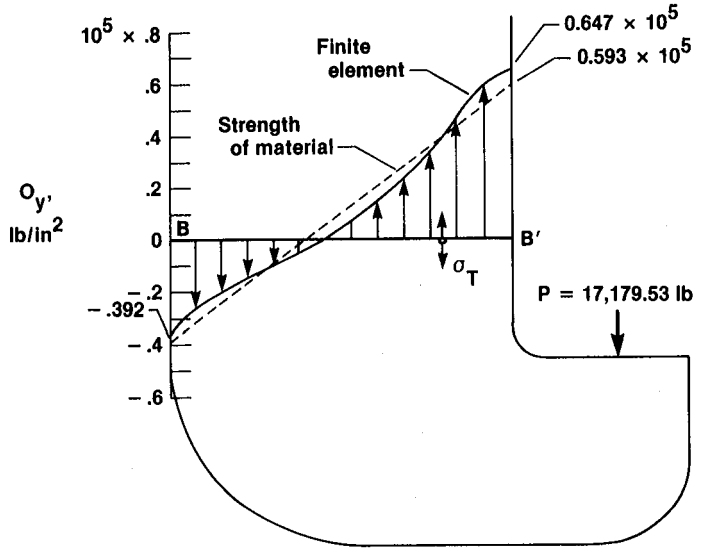

Figure 12. Distribution of σ_T along B–B′ (old rear hook, P = 17,179.53 lb).

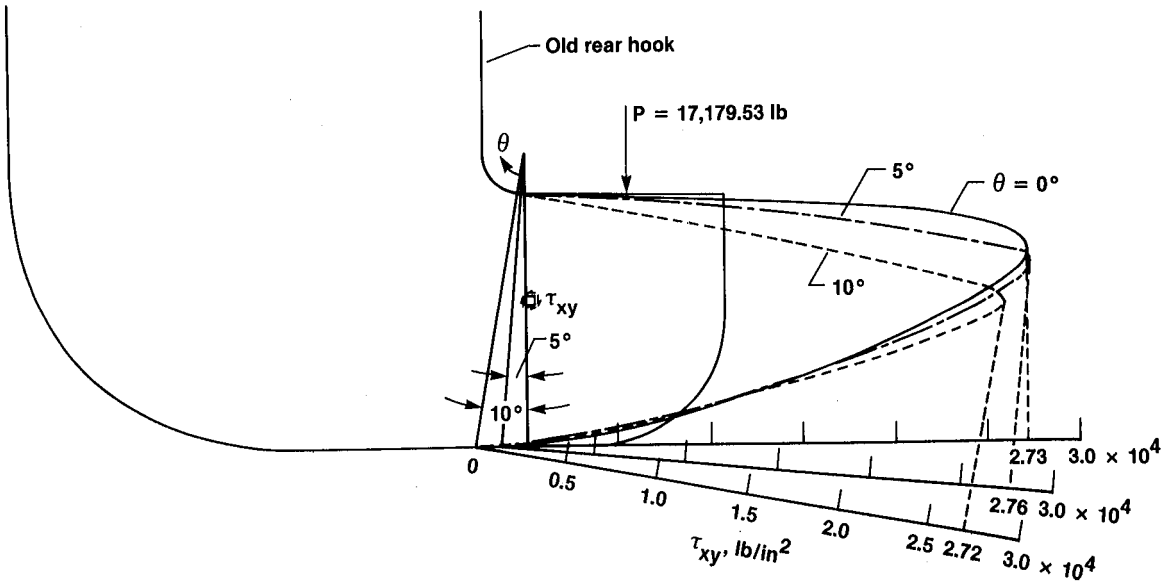

Figure 13. Distribution of shear stress τ_{xy} along Θ = 0°, 5°, and 10° lines for P = 17,179.53 lb (old rear hook).

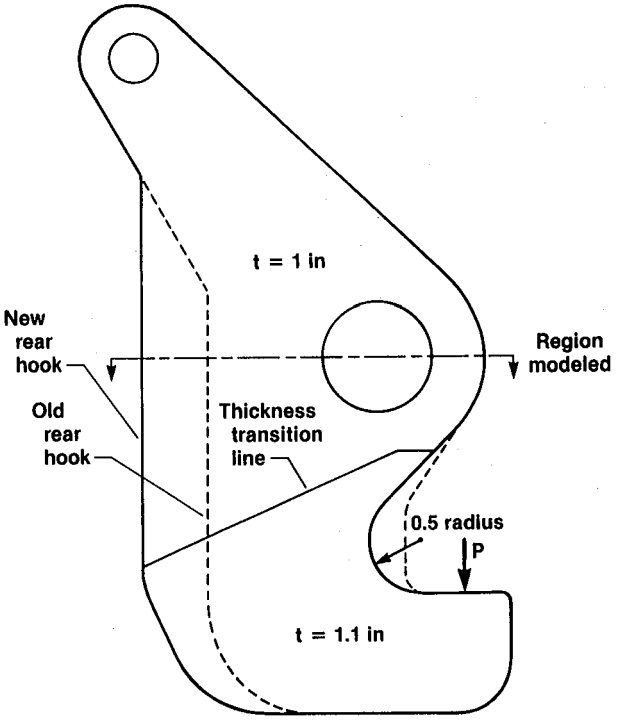

Figure 14. Geometry of B-52 pylon new rear hook.

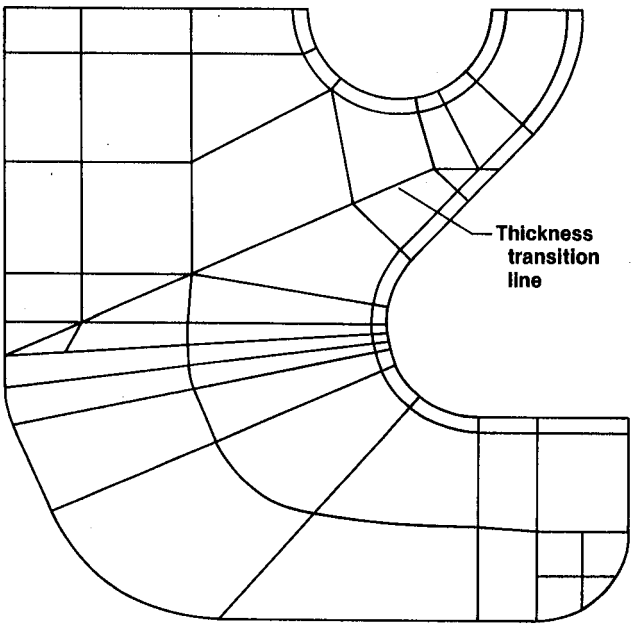

Figure 15. PATRAN patches (subregions) for generating meshes for the new rear hook NASTRAN model.

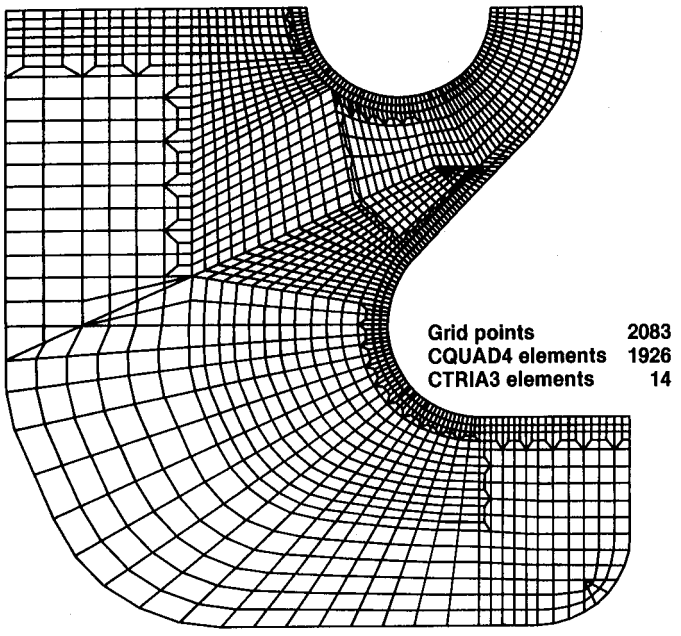

Figure 16. New rear hook NASTRAN model.

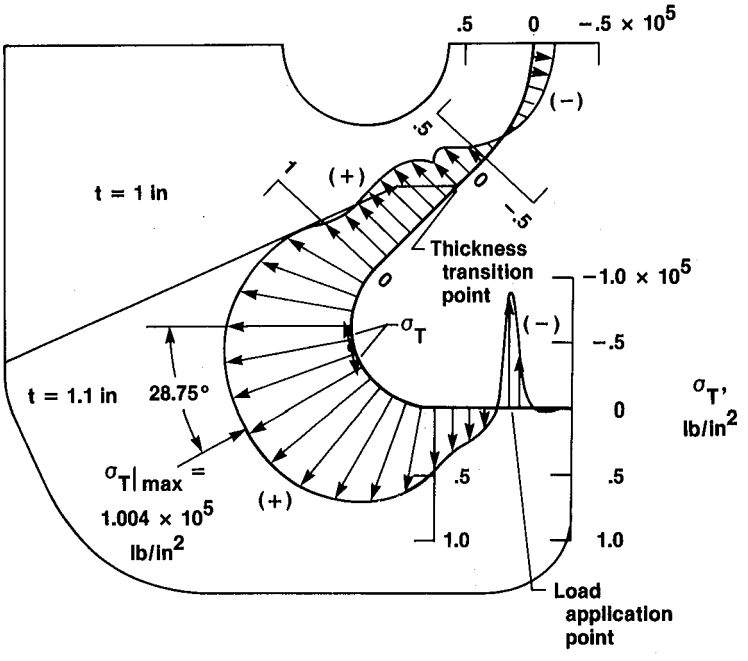

Figure 17. Distribution of tangential stress σ_T along inner boundary of the new rear hook (AMAX MP35N steel alloy, P = 17,179.53 lb).

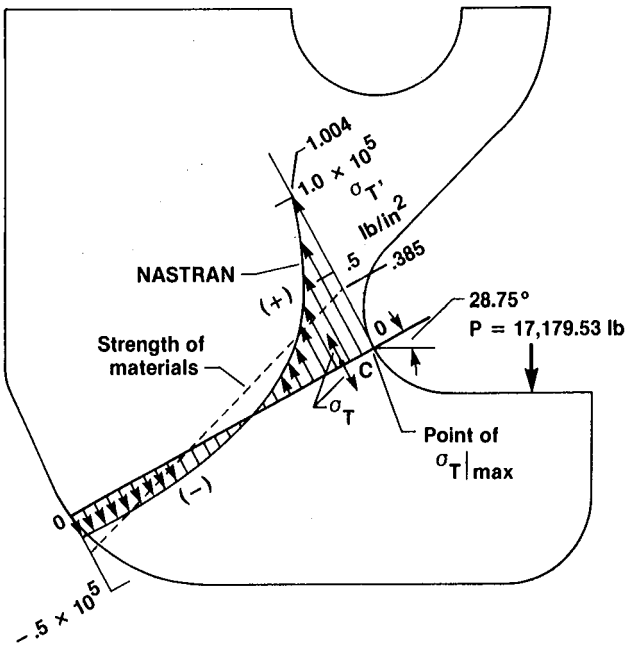

Figure 18. Distribution of σ_T along line B-B for 17,179.53 lb load (new rear hook).

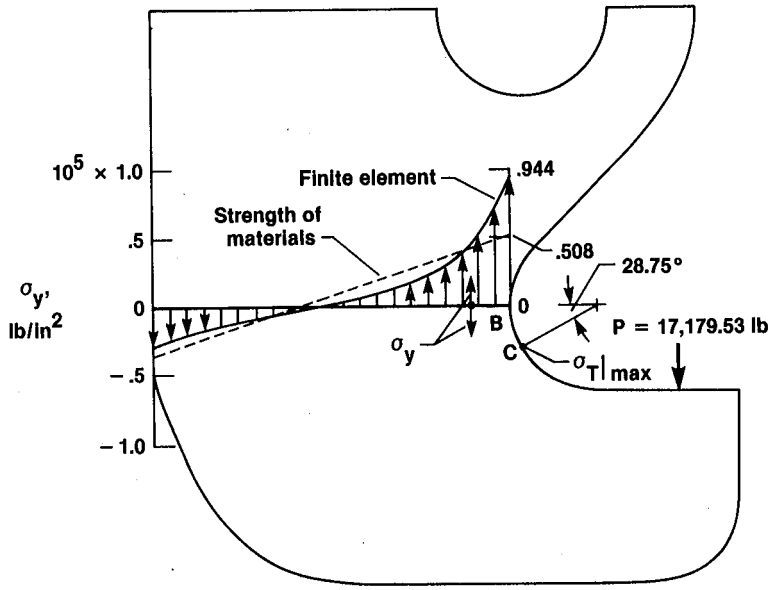

Figure 19. Distribution of normal stress σ_y along A-A in the new rear hook (AMAX MP35N steel alloy, P = 17,179.53 lb).

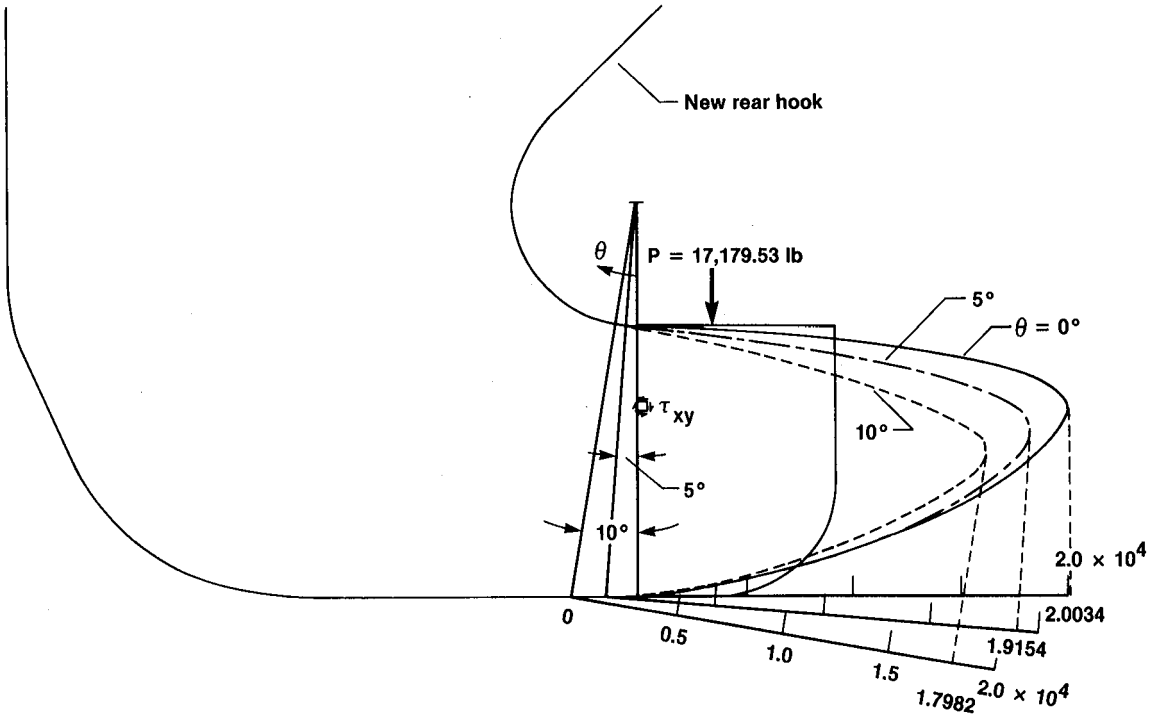

Figure 20. Distribution of shear stress τ_{xy} along Θ = 0°, 5°, and 10° lines for P = 17,179.53 lb (new rear hook).

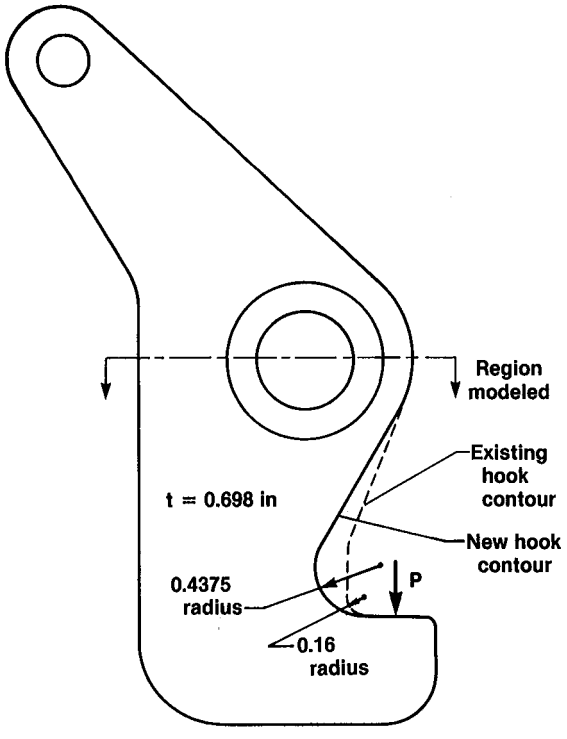

Figure 21. Geometry of B-52 pylon new DAST rear hook.

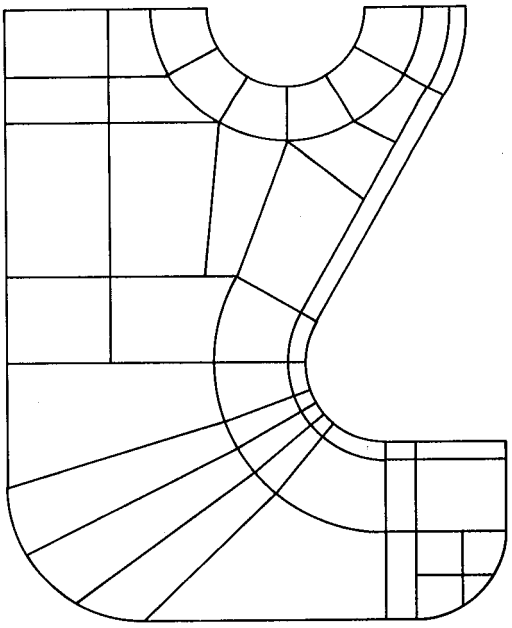

Figure 22. PATRAN patches (subregions) for generating meshes for the new DAST rear hook NASTRAN model.

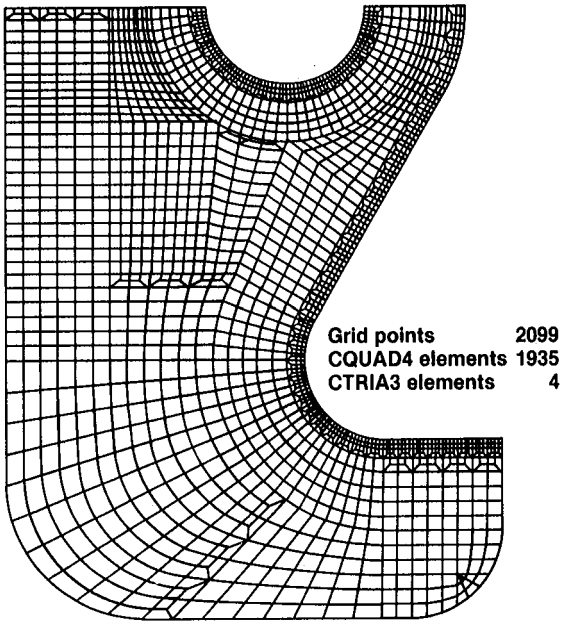

Figure 23. New DAST rear hook NASTRAN model.

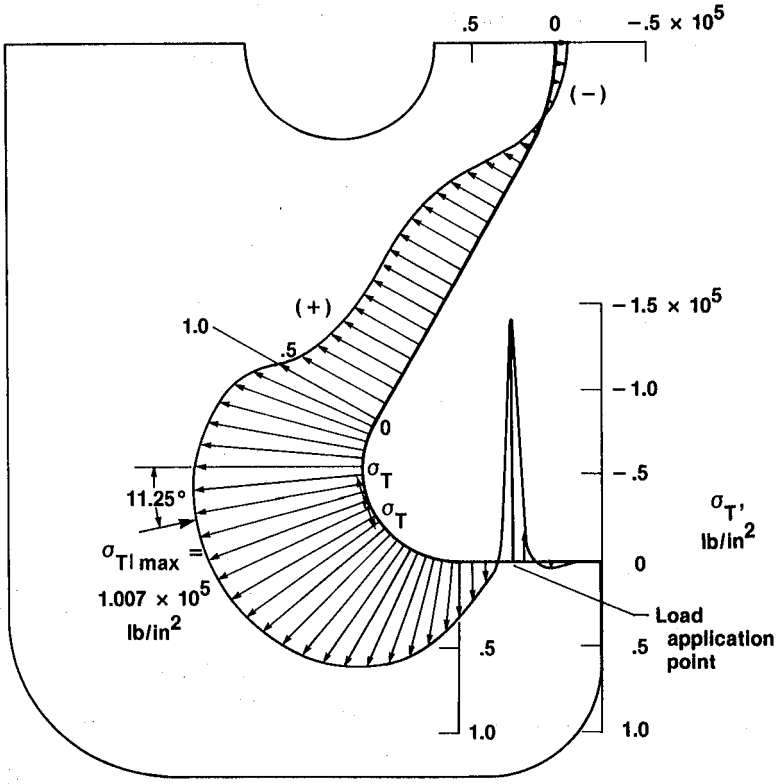

Figure 24. Distribution of tangential stress σ_T along inner boundary of the new DAST rear hook for P = 10,000 lb load.

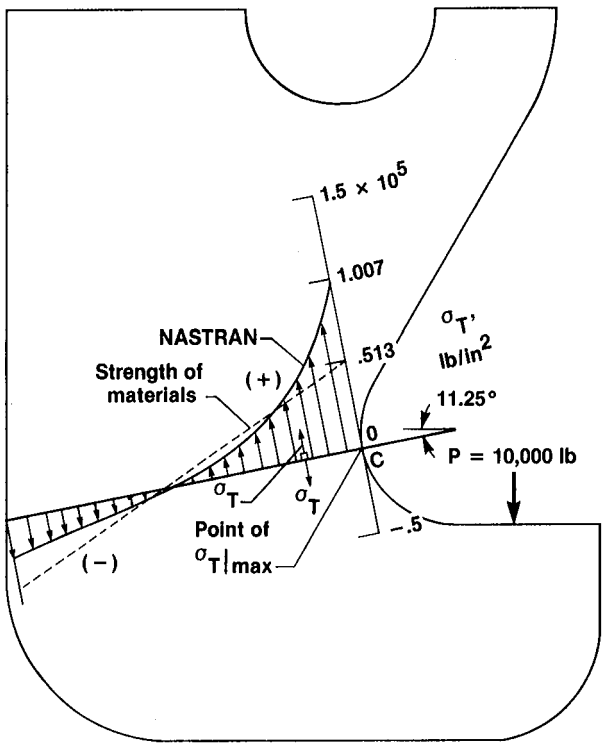

Figure 25. Distribution of σ_T along line 0-0 for 10,000-lb load (new DAST rear hook).

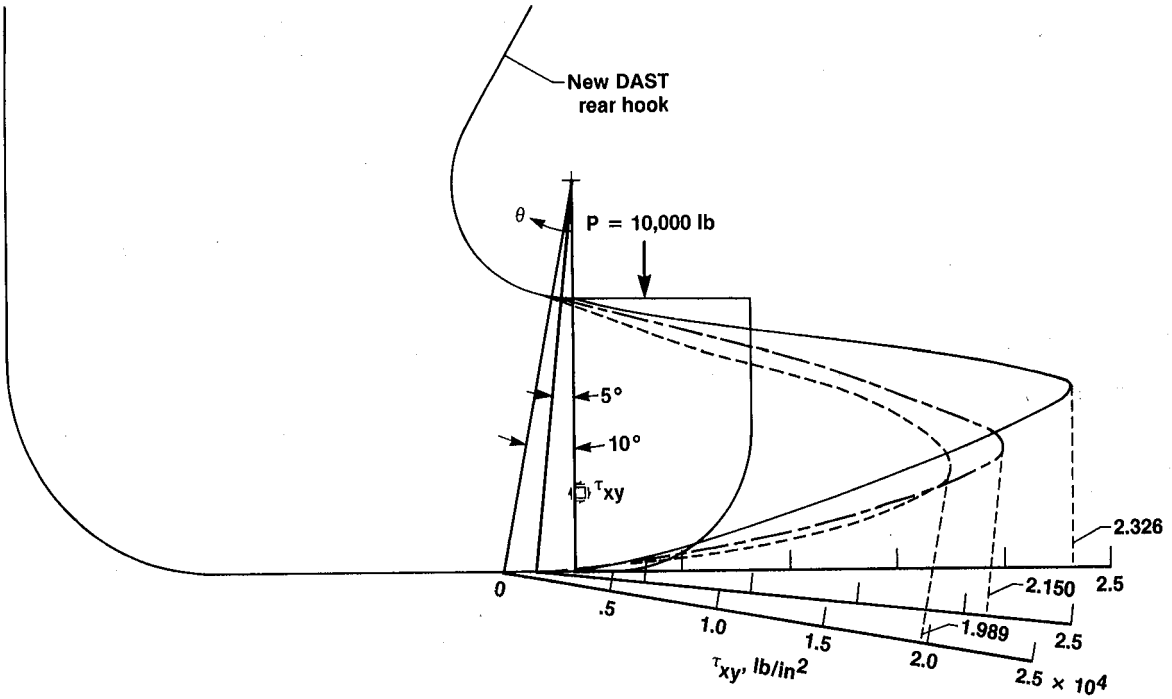

Figure 26. Distribution of shear stress τ_{xy} along Θ = 0°, 5°, and 10° lines for P = 10,000-lb load (new DAST rear hook).

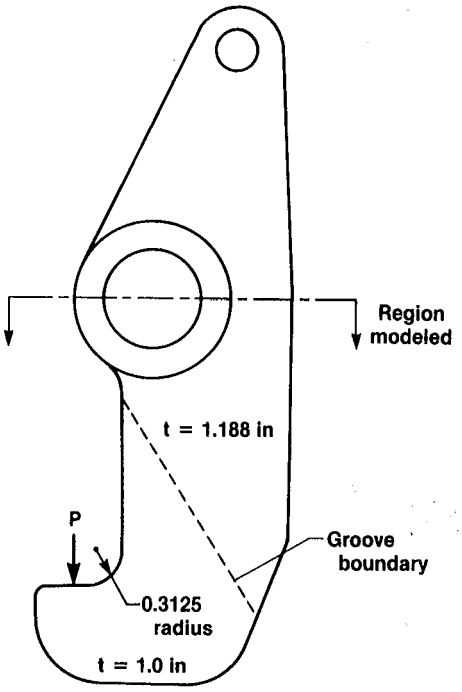

Figure 27. Geometry of B-52 pylon front hook.

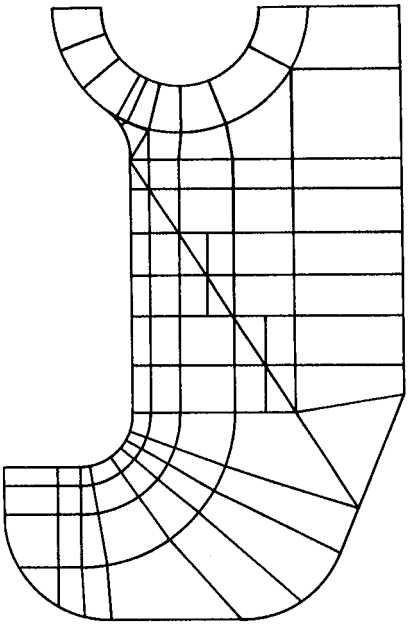

Figure 28. PATRAN patches (subregions) for generating meshes for the front hook NASTRAN model.

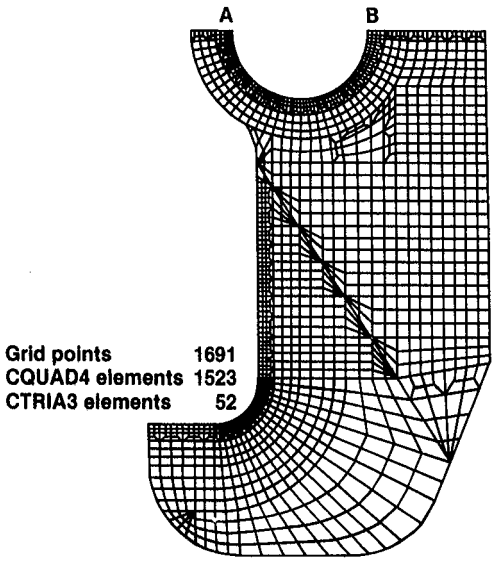

Figure 29. Front hook NASTRAN model.

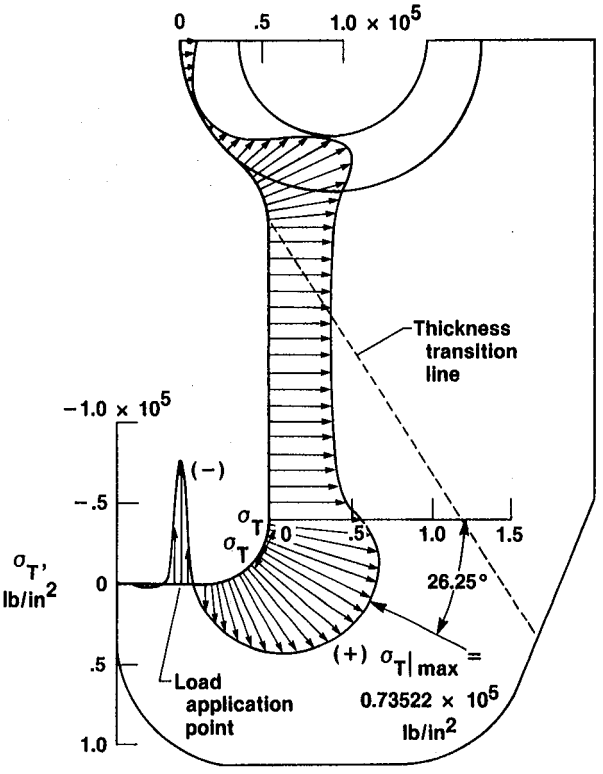

Figure 30. Distribution of tangential stress σ_T along inner boundary of the front hook P = 10,000 lb.

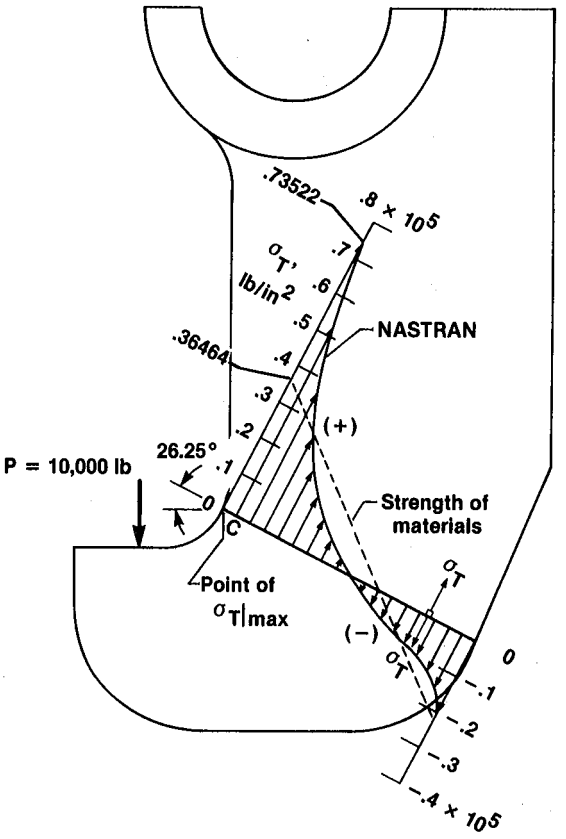

Figure 31. Distribution of σ_T along line 0-0 for 10,000-lb load (front hook).

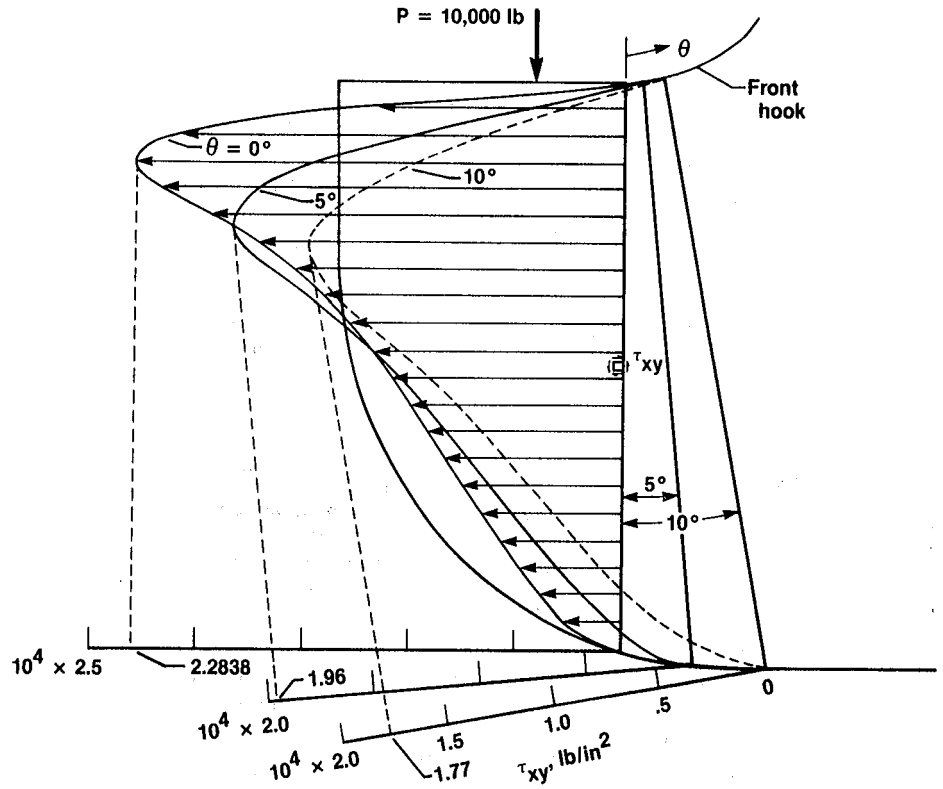

Figure 32. Distribution of shear stress τ_{xy} along $\theta = 0°$, 5°, and 10° lines for P = 10,000-lb load (front hook).

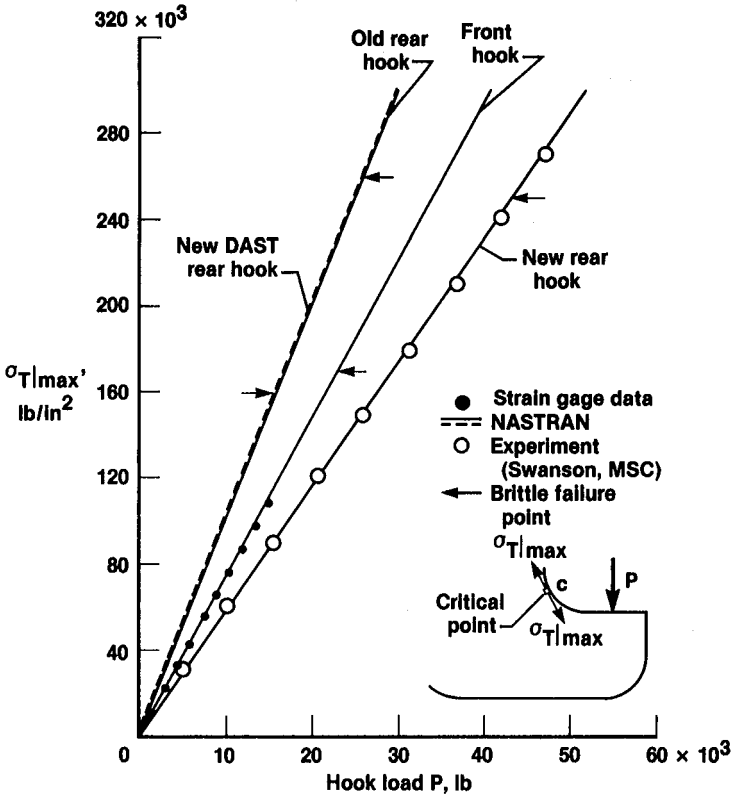

Figure 33. Hook loads as a function of maximum tangential stresses at the critical points of the hooks.

1. Report No. NASA TM-84924	2. Government Accession No.	3. Recipient's Catalog No.
4. Title and Subtitle Stress Analyses of B-52 Pylon Hooks		5. Report Date October 1985 6. Performing Organization Code H-1221
7. Author(s) William L. Ko and Lawrence S. Schuster		8. Performing Organization Report No. 10. Work Unit No.
9. Performing Organization Name and Address NASA Ames Research Center Dryden Flight Research Facility P.O. Box 273 Edwards, CA 93523		11. Contract or Grant No. 13. Type of Report and Period Covered Technical Memorandum
12. Sponsoring Agency Name and Address National Aeronautics and Space Administration Washington, D.C. 20546		14. Sponsoring Agency Code RTOP 505-43-31

15. Supplementary Notes

16. Abstract

The NASTRAN finite element computer program was used in the two-dimensional stress analysis of B-52 carrier aircraft pylon hooks: (1) old rear hook (which failed), (2) new rear hook (improved geometry), (3) new DAST rear hook (derated geometry), and (4) front hook. NASTRAN model meshes were generated by the aid of PATRAN-G computer program. Brittle limit loads for all the four hooks were established. The critical stress level calculated from NASTRAN agrees reasonably well with the values predicted from the fracture mechanics for the failed old rear hook.

17. Key Words (Suggested by Author(s))	18. Distribution Statement
B-52 pylon hooks PATRAN mesh generations NASTRAN stress analysis Stress concentrations Fracture mechanics	Unclassified – Unlimited STAR category 39

19. Security Classif. (of this report)	20. Security Classif. (of this page)	21. No. of Pages	22. Price*
Unclassified	Unclassified	31	A03

For sale by the National Technical Information Service, Springfield, Virginia 22161.